# Hydrogen gas sensor utilizing a high proton affinity of *p*-diketodipyridylpyrrolopyrrole

*H. Takahashi and J. Mizuguchi; Graduate School of Engineering, Yokohama National University; 79-5 Tokiwadai, Hodogaya-ku, 240-8501 Yokohama, Japan*

## Abstract

*Organic pigments were once extensively investigated as photoconductors for the electrophotographic photoreceptor. Nowadays, they play an important role as colorants for color copies as well as materials for optical discs, electroluminescence, FET etc. Here, we report another novel application of organic pigments for $H_2$ gas sensors. A high-performance hydrogen gas sensor has been developed that utilizes a proton affinity of 1,4-diketo-3,6-bis-(4'-pyridyl)-pyrrolo-[3,4-c]-pyrrole (DPPP) known as a red pigment. We found that the N atom of the pyridyl ring of the DPPP can easily be protonated by protons dissociated from $H_2$ to induce a remarkable change in electrical conductivity by several orders of magnitude. The appealing feature of the device is the reversible operation at room temperature as characterized by a change in electrical resistivity by two orders of magnitude even under 0.05 % $H_2$.*

## 1. Introduction

1,4-Diketo-3,6-diphenyl-pyrrolo-[3,4-*c*]-pyrrole (DPP: Fig. 1(a)) and its derivatives are industrially important red pigments used as colorants in painting industries as well as in imaging areas.[1)] Among these, a derivative with pyridyl rings (DPPP: diketodipyridylpyrrolopyrrole; Fig. 1(b)) is known to exhibit a high tinctorial strength of the red color in powders and possesses a high weatherfastness. However, the color suddenly changes from vivid red to dull red when a pigment-dispersed layer in polymers was prepared at elevated temperatures. Our in-depth study clarified that traces of protons are liberated from the polymer matrix at high temperatures and then protonates DPPP at the N atom of the pyridyl ring.[2)]

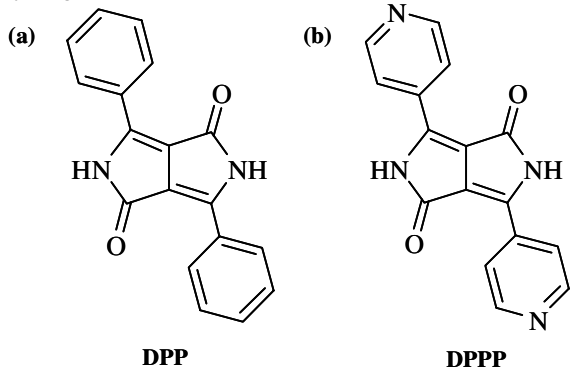


**Fig. 1:** *Molecular conformation: (a) DPP and (b) DPPP.*

Our model experiment based on the vapor of nitric acid shows the spectral change as shown in Fig. 2(a).[2] To our great surprise, the electrical resistivity decreases remarkably due to protonation by five orders of magnitude (Fig. 2(b)), also accompanied by the appearance of photoconduction. On the basis of the present outstanding effect, we firmly believed that we could develop a sensitive $H_2$-sensor by making use of a high proton affinity of DPPP. Then, our attention was focused on how to dissociate $H_2$ into protons. We have solved this problem by incorporating Pd or Pt layers into the sensor element. The $H_2$ sensor which we have successfully developed operates at room temperature in the following sequence: the first step is the dissociation of $H_2$ by means of a sputtered Pd-layer. The second sequence involves proton capture by the N atom of the pyridyl ring (proton acceptor) that releases an electron, leading to the changes in electrical conductivity.

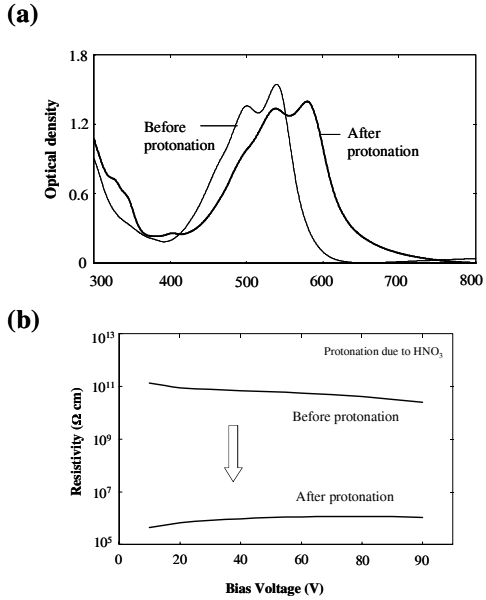


**Fig. 2:** *(a) Absorption spectra and (b) change in resistivity before and after protonation.*

## 2. Experiment

### *2-1. Operation principle of the $H_2$ sensor*[3, 4)]

Fig. 3(a) shows the interdigital electrodes made of Al or ITO (Indium-Tin-Oxide) which were prepared by lithographic technique. The sensor based on the interdigital electrodes must include two important functions: one is to dissociate $H_2$ into protons and the other is to detect the change in electrical conductivity due to protonation. In order to dissociate $H_2$, we incorporate a thin layer of Pd, Pt, or Pd/Pt since $H_2$ is known to be unstable on these metals. At the same time, we apply a rather high electric field between electrodes in order to assist the dissociation of $H_2$. The successful

result is obtained by sputtering Pd or Pt directly on the interdigital electrodes to avoid their contacts in the form of islands as shown in Fig. 3(b), followed by application of DPPP by vacuum evaporation. Since $H_2$ is fist adsorbed on the surface of DPPP and its subsequent dissociation follows underneath the DPPP layer due to Pd, the DPPP layer must be thin enough to detect the change in electrical conductivity due to protonation. The optimum thickness of Pd layer is about 3 Å while DPPP is deposited to the thickness of about 300 Å.

Al and ITO work equally good as the electrode. Furthermore, no significant difference is recognized in dissociation ability of $H_2$ between Pd, Pt, and Pd/Pt. Therefore, in the present report, the result is given for the device which includes ITO electrode used in combination with sputtered Pd. The device structure is ITO/sputtered-Pd/DPPP/ITO on the basis of the interdigital electrodes (Fig. 3).

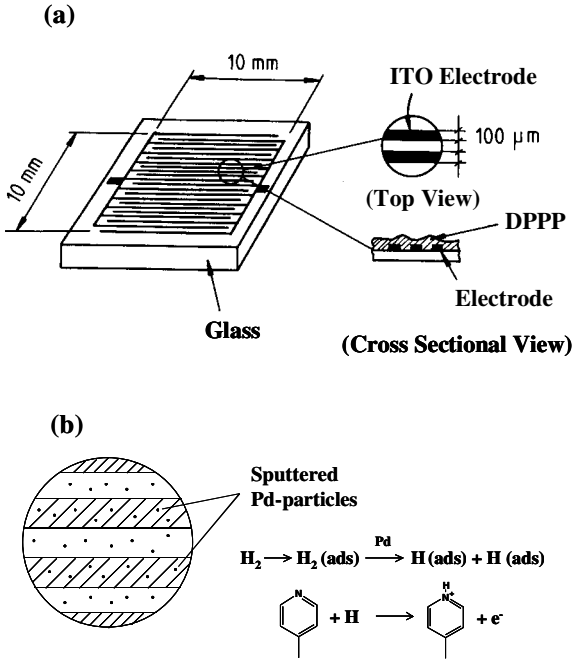


**Fig. 3:** *(a) Interdigital electrodes and (b)magnified Pd-sputtered electrodes.*

### 2-2. Synthesis and crystal phase used for the sensor

There are two crystal modifications in DPPP: phase I (grown from vapor phase )[5] and phase II ( recrystallized from solution).[6] The projection of the crystal structure onto the molecular plane is shown in Fig. 4 for phases I and II. A striking difference is recognized between two modifications in the hydrogen bond network. Phase I is uniquely characterized by NH···O intermolecular hydrogen bonds between the NH group of one molecule and the O atom of the neighboring one. On the other hand, there exists another type of NH···N hydrogen bonds in phase II in addition to the NH···O bond. This NH···N bond is formed between the NH group of one molecule and the N atom of the pyridyl ring of the neighboring one. In phase I, two N atoms of the pyridyl ring remain free (*i.e.* unbonded) while one of the N atom is blocked by the NH···N hydrogen bond in phase II.

Therefore, phase I is obviously more appropriate for $H_2$ sensors because two N atoms are available as the proton acceptor. Luckily enough, phase I is the phase as obtained by vacuum evaporation.

## 3. Results and Discussion

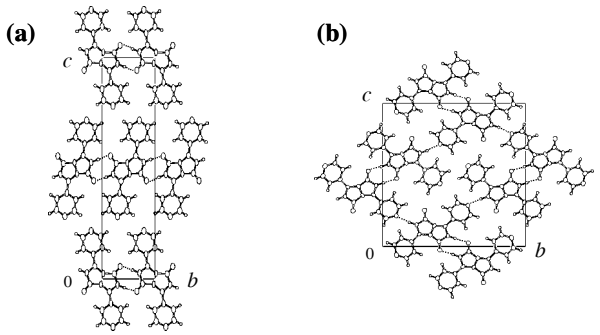


**Fig. 4:** *Projection of the crystal structure.*

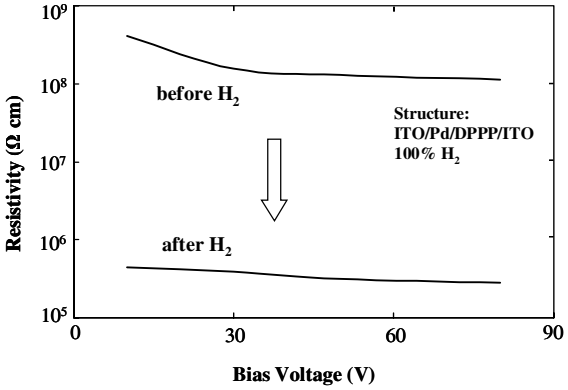


**Fig. 5:** *Change in resistivity of the sensor.*

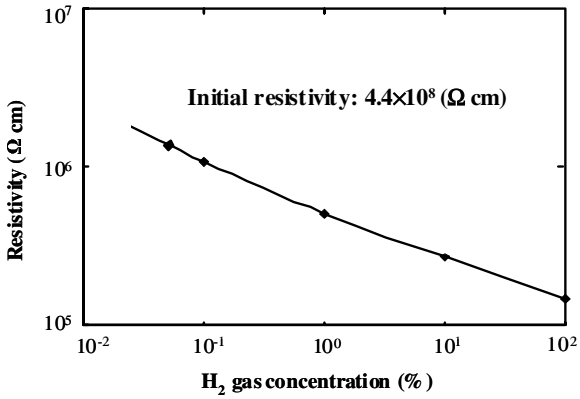


**Fig. 6:** *Log-Log plot of the resistivity and $H_2$ concentration.*

### 3.1 Performance of the $H_2$ gas sensor

Fig. 5 shows the change in resistivity of the sensor as a function of bias voltage when the sensor is exposed to 100% $H_2$. The resistivity decreases drastically by three orders of magnitude at room temperature. The resistivities for the $H_2$ concentrations of 0.05, 0.1, 1 and 10 % are shown in Fig. 6. It is remarkable to note

that the resistivity diminishes by two orders of magnitude even for the $H_2$ concentration of 0.05 %. Furthermore, the resistivity is found to decrease linearly with increasing $H_2$ concentration, since Fig. 6 is a log-log plot of the resistivity and $H_2$ concentration. Fig. 7 shows the build-up of the sensor signals as a function of time. The build-up time (80% of the maximum value) is about 400 ms where the gain is *ca* 900.

This indicates that the response is quite rapid in the gain range of several factors. The signal builds up and builds down and then remains nearly constant. When $H_2$ is switched off, the signal decays and comes back to the initial state in five minutes. The return process is rather slow, but is still reversible a high sensitivity.

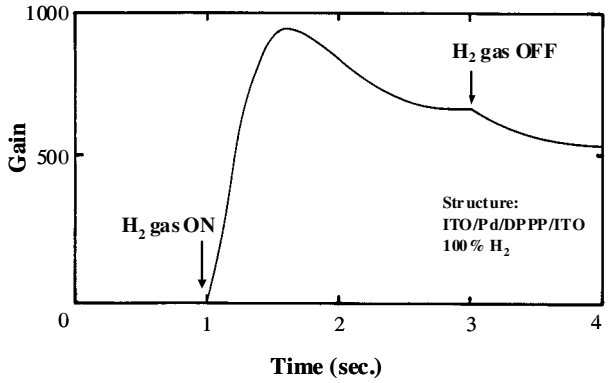


**Fig. 7:** *Build-up of the sensor signal as a function of time.*

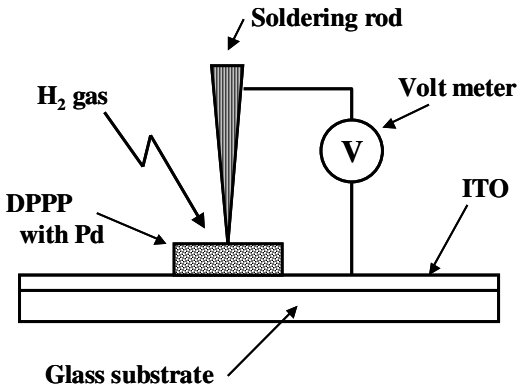


**Fig. 8:** *Experimental setup for measurements of the Seebeck coefficient.*

### 3-2. Determination of charge carriers

In general, carrier determination in highly resistive materials is not an easy task because the number of charge carriers is quite small. Organic pigments such as DPPP falls in this category that has a resistivity of about $10^{11}$ Ωcm. For these materials, a thermoelectric power method based on the Seebeck effect is sometimes helpful. Fig. 8 shows the experimental setup for the determination of charge carriers on the basis of the Seebeck effect. A soldering rod was used as the heating element as well as the counter electrode to measure thermoelectromotive force that appears due to a temperature difference between two electrodes through DPPP.

An *n*-type Si chip was used as the reference. If the potential at the soldering rod appears positive, the charge carrier is then determined to be electrons. On the contrary, the carrier is holes if the potential is negative. Three kinds of samples were prepared: evaporated DPPP, evaporated/protonated DPPP and $H_2$ gas sensor based on DPPP. The evaporated/protonated DPPP serves as a model substance for the $H_2$ gas sensor.

Fig. 9 shows the thermoelectric power *vs* time for DPPP alone, protonated DPPP as well as $H_2$ gas sensor under 100 % $H_2$. The magnitude of the signals depends largely on the geometry of the samples (see Experiment). A positive potential appears in all samples at the hot end, indicating clearly that the charge carriers are attributed to electrons. Although the thermoelectric power in $H_2$ gas sensor is small, it is evident that the potential is positive at the hot end and that the charge carriers are again due to electrons. The present result directly bears out the operation principle shown in Fig. 3.

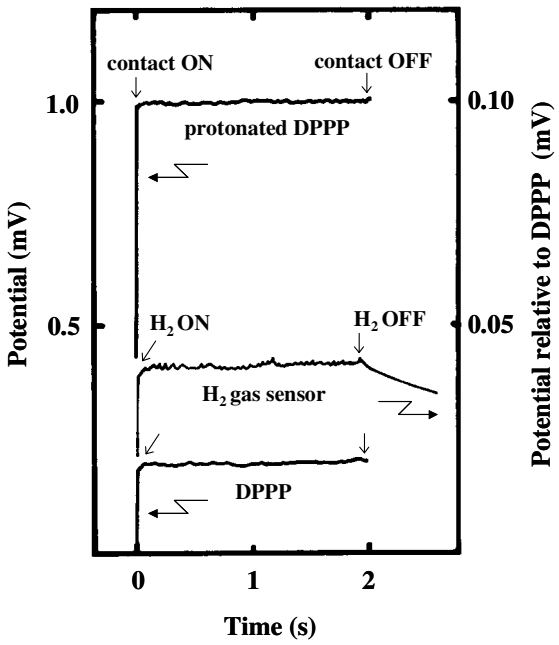


**Fig. 9:** *Themoelectric power observed along the direction of the temperature gradient: evaporated DPPP, evaporated/protonated DPPP and $H_2$ gas sensor (see text) under 100 % $H_2$. The potential for the $H_2$ gas sensor is plotted relative to DPPP. The positive potential always appear in all samples at the hot end, indicating an electron conduction.*

### 3-3. Influence of various gases on the gas sensor

We have studied the influence of various gases on the sensing characteristic: $CH_4$ (1 %), CO (2 %), $CO_2$ (24 %), NO (0.6 %) and $SO_2$ (0.2 %) and $H_2O$ moisture. The sensor was exposed to these gases with a flow rate of 2 l/min. No noticeable effect (*i.e.* less than 0.1 % in resistivity change) was recognized for these gases, indicating that the sensors are free from the influence of ambient gases.

### 3-4. Performance of DPPP isomers: o- and m-DPPP

We have also characterized *o*- and *m*-DPPPs for $H_2$ sensors.[7)]

Quite contrary to our expectation, the sensors based upon *o*- and *m*-DPPPs exhibit extremely poor sensitivity as compared with that of *p*-DPPP. Structure analysis of *o*- and *m*-DPPPs[8, 9] revealed that the N atom of the pyridyl ring, *i.e.* the antenna part of the $H_2$ sensor, is found to be totally blocked by the formation of NH···N intermolecular hydrogen bond between the NH group of *o*- or *m*-DPPP and the N atom of the neighboring molecule. That is, the N atom is entirely used up for the formation of NH…N hydrogen bonds. This interprets why *meta*-DPPP gives a poor sensitivity against $H_2$.

### *3-5 Extension to other pigments*

A further trial has been made to integrate pyridyl rings in perylene-imides[10] as well as in Cu-phthalocyanine[11]. The sensitivity in these sensors is found to be higher by one order of magnitude than that of DPPP. In addition, the build-up and the build-down characteristics are significantly faster than that of DPPP.

## 4. Conclusions

A high-performance $H_2$ gas sensor has been developed on the basis of diketodipyridylpyrrolopyrrole derivatives. The sensing operation involves proton capture by DPPP which releases an electron, leading to the changes in the electrical resistivity. A reduction of resistivity by two orders of magnitude is achieved at room temperature for 0.05 % $H_2$. The process is reversible and the response time is about 400 m*s*. Furthermore, no noticeable effect of ambient gases ($CH_4$, CO, $CO_2$, NO and $SO_2$ gases together with $H_2O$ moisture) is found on the present sensor.

## References


1) M. Herbst and K. Hunger, Industrial Organic Pigments, pp.550-553, VCH, Weinheim, (1993).

2) J. Mizuguchi: "Solution and solid state properties of 1,4-diketo-3,6-bis-(4'-pyridyl)-pyrrolo-[3,4-*c*]-pyrrole on protonation and deprotonation", Ber. Bunsenges. Phys. Chem., **97**, 684 (1993).

3) H. Takahashi and J. Mizuguchi: "Hydrogen gas sensor utilizing a high proton affinity of pyrrolopyrrole derivatives", J. Electrochem. Soc. 152, H69 (2005).

4) H. Takahashi and J. Mizuguchi: Carrier generation and carrier determination in dipyridyldiketopyrrolopyrrole-based $H_2$ gas sensors, J. Appl. Phys. **100**, 034908(1)-034908(6) (2006).

5) J. Mizuguchi, T. Imoda, H. Takahashi and H. Yamakami: "Polymorph of 1,4-diketo-3,6-bis –(4'-dipyridyl)-pyrrolo-[3,4-*c*]-pyrrole and their hydrogen bond network: A material for $H_2$ gas sensor" , Dyes and Pigments, **68**, 47 (2005).

6) J. Mizuguchi, H. Takahashi and H. Yamakami: "Crystal structure of 3,6-bis(4'-pyridyl)-pyrrolo [3,4-*c*]-pyrrole-1,4-dione, $C_{16}H_{10}N_4O_2$ at 93K", Z. Kristallogr. NCS, **217**, 519 (2002).

7) T. Hirota, T. Imoda, H. Takahashi and J. Mizuguchi: Correlation between $H_2$ gas sensitivity and structure of *o*-, *m*-, and *p*-dipyridyldiketopyrrolopyrroles as viewed from the electron delocalization within the molecule and the crystal structure, J. Imag. Soc. Jpn. **45**, 328-336 (2006).

8) J. Mizuguchi, T. Imoda and H. Takahashi: 3,6-Di-4-pyridylpyrrolo[3,4-*c*]pyrrole-1,4(2*H*,5*H*)-dione, Acta Cryst. **E61,** o500-o502 (2005).

9) T. Imoda, T. Hirota, H. Takahashiand J. Mizuguchi,: 3,6-Di-2-pyridylpyrrolo[3,4-*c*]pyrrole-1,4(2*H*,5*H*)-dione, Acta Cryst. **E61,** o616-o618 (2005).

10) K. Sato, K. Hino, H. Takahashi and J. Mizuguchi: Hydrogen gas sensor based upon perylene-imide derivatives, IJISTA Int. J. Intell. Sys. Technol. Appl. **3**, 52-62 (2007).

11) T. Hoki, H. Takahashi, S. Suzuki, and J. Mizuguchi: Hydrogen Gas Sensor based upon proton acceptors integrated in Copper-tetra-2,3-pyridinoporphyradine, IEEE Sensors J. (2007) in print.


## Author Biography


*Hiroo Takahashi received his Bachelor of Engineering from Waseda University in 1968 and Dr. of Engineering from Yokohama National University in 2005. He worked at Sony Corporation from 1968 to 2004. He was involved in R&D of Trinitron TV from 1968 to 1975 as a senior manager, as well as of optical discs from 1975 to 2004 as the general manager. He is currently a visiting scientist at the Yokohama National University. E-mail: Mizu-j@ynu.ac.jp*